

Multifunctional Lipophobic Polymer Dots from Cyclodextrin: Antimicrobial/Anticancer Laborers and Silver Ions Chemo-Sensor

Albandary Almahri, Ameena M. Al-bonayan, Roba M. S. Attar, Alaa Karkashan, Basma Abbas, Salhah D. Al-Qahtani, and Nashwa M. El-Metwaly*



Cite This: *ACS Omega* 2023, 8, 16956–16965



Read Online

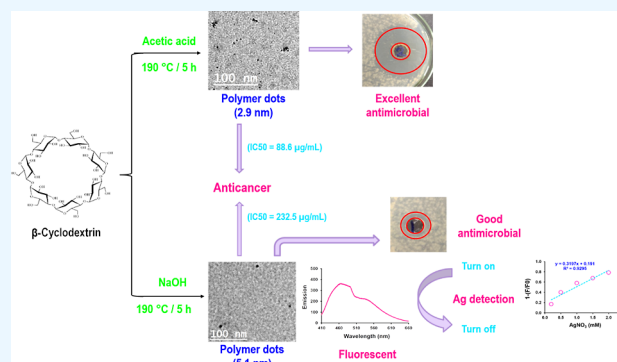
ACCESS |

Metrics & More

Article Recommendations

Supporting Information

ABSTRACT: β -Cyclodextrin (CD) is currently exploited for the implantation of lipophobic polymer dots (PDs) for antimicrobial and anticancer laborers. Moreover, the PDs were investigated to act as a chemo-sensor for metal detection. The data revealed that under basic conditions, photoluminescent PDs (5.1 nm) were successively clustered with a controllable size at 190 °C, whereas under acidic conditions, smaller-sized non-photoluminescent carbon nanoparticles (2.9 nm) were obtained. The fluorescence intensity of synthesized PDs under basic conditions was affected by pH, and such an intensity was significantly higher compared to that prepared under acidic conditions. The PDs were exploited as florescent detectors in estimation of Ag^+ ions in aquatic streams. Treatment of Ag^+ ion colloids with PDs resulted in fluorescence quenching attributing to the production of AgNPs that approved by spectral studies. The cell viability percent was estimated for *Escherichia coli*, *Staphylococcus aureus*, and *Candida albicans* after incubation with PDs implanted under basic conditions for 24 h. The cell mortality percent was estimated for breast cancer (MCF-7) after incubation with different concentrations of PDs that were implanted under acidic versus basic conditions to show that treatment of the tested cells with 1000 $\mu\text{g}/\text{mL}$ PDs prepared under basic (IC₅₀ 232.5 $\mu\text{g}/\text{mL}$) and acidic (IC₅₀ 88.6 $\mu\text{g}/\text{mL}$) conditions resulted in cell mortality percentages of 70 and 90%, respectively.



1. INTRODUCTION

Polymer dots (PDs) are ascribed as one of the recently investigated members of carbon quantum dots (CQDs), ingrained from carbon enriched polymeric skeletons, decorated with heteroatoms containing functional groups.^{1–3} PDs are known to exhibit a spherical-like topography, with a particle size less than 10 nm, to be characterized with more intriguing properties compared with the other carbon nanostructures.⁴ These lead to make PDs act as superior alternatives for the other members of carbon nanostructures.^{5–7} Numerous reports were considerably interested in investigating of green costless techniques for nucleation of CQDs owing to their superiorly characteristic activities, like being chemically inert, photoluminescence, cost effectiveness, bio-competence, and abundance of the starting equivalents.^{8–14}

Fluorescent CQDs are exhibited with excellency over the other metallic nanoparticles in different purposes owing to their low toxic effects, biocompatibility, and biodegradability.^{4,15–17} Therefore, it was exploited as good alternatives for metallic-based nanostructures in drug delivery, bio-sensing, bio-imaging, optoelectronic devices, photodynamic therapy, photo-catalysis, electro-catalysis, and chemical sensing.^{18,19}

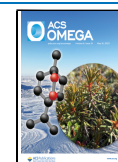
Polysaccharides as organic biopolymers could be described as good starting materials for the nucleation of PDs with an

active surface decorated with heteroatom-containing functional groups. Meanwhile, starting with polysaccharides for clustering of PDs is known suitable for surface decoration with oxygen/nitrogen or sulfur-containing moieties, reflecting in acquiring the ingrained PDs, the water hydrophilicity, and the opportunity for further modifications.²⁰ For controllable geometry and size distribution, different synthesis methodologies were studied in order to proceed as a simple, less expensive, and energy saving-large scale approach. Altering the experimental factors such as reaction duration and temperature also described as key parameters for adjusting the topography and size average of the ingrained PDs. All of the recent studies that demonstrated various synthetic methodologies are generally categorized into two main techniques as top-down such as oxidation^{21–23} and electro-chemical technique^{24,25} and bottom-up such as the hydrothermal approach^{26–28} and microwave-assisted technique.^{29,30}

Received: February 10, 2023

Accepted: April 21, 2023

Published: May 8, 2023



Cyclodextrins (CDs) are prepared via enzymatic modification of starch to be composed of six, seven, or eight glucopyranoside units (α , β , and γ CD, respectively) chemically bonded together via an α -(1–4) ether linkages.^{31,32} The arrangement of the glucopyranose moieties results in preparation of a cyclic oligosaccharide with a lipophilic central cavity. This characteristic structure promotes them to form a stable inclusion complex with a wide variety of guesting hydrophobic moieties.³³ Therefore, PDs nucleated from CDs could be ascribed as excellent candidates for the preparation of selective and sensitive nano-objects for different targets since it could be concurrently exhibited with the molecular recognition properties of CDs and the optical activities of QDs.³⁴ According to literature, chemical sensors based on natural and derivative CD-capped QDs were synthesized for biomedical and environmental purposes.^{34–37} Among all types of CD, β -CD is the most commercially available one and its cavity is characterized with adequate size to have stable inclusion complexes for a wide variety of guesting molecules especially the drugs. However, it exhibited with the disadvantageous property of scarce water solubility (1.85 g/100 mL, at 25 °C).³⁸

Various laborers were exploited as antiseptics and disinfectants for the inactivation of microorganisms to prohibit their dangerous infectious actions;^{39–42} however, these antimicrobial agents were disadvantageous with toxic effects and extreme irritation, leading to risky effects like dermatotic contact and mucous membrane irritating. Moreover, some of the exposed microbes can adapt and show some resistance.⁴³ Therefore, investigating of PDs as superior microbicidal laborers with high potentiality and low toxic effects is importantly required and considerably concerned.

On the other hand, PDs could be considerably exploited as good laborers as metal detectors attributing to its biocompetence. Whereas, some of heavy metals, such as zinc or iron, are vitally required for human body and are shown with low harmful effects in its limited concentrations, while they have important effects in metabolism. On the other hand, some heavy metals are very risky for human health although it exists as traces, such as Hg, Pb, and Cd.^{44,45} These harmful metals could be easily collected within the body and to be coordinately interacted with the enzymes and nucleic acids, leading to corruption of their normal functions.^{45,46} Herein, a unique and green procedure is investigated for nucleation of lipophobic PDs using β -CD. The clustered PDs were exploited as probing reagents for environmental applications to be applicable as a microbicidal reagent and fluorescent silver ions detector in addition to be superiorly applied as anti-inflammatory laborer. The current approach is performed under hydrothermal conditions as a comparative study to demonstrate the efficiency of CD as starting equivalent for PDs under acidic versus basic conditions, taking in account the effect of reaction temperature in nucleation of the desired nanodots. Dialysis as a step of ultra-purification of the ingrained PDs was performed for obtaining mono-dispersed PDs. The affinity of the current approach in nucleation of PDs was confirmed via different instruments like UV–visible spectroscopic analysis, transmission electron microscopy (TEM), FTIR, ¹H NMR, and ¹³C NMR. Consequently, the photoluminescence of the clustered PDs was also studied, while the superiority in optical sensitiveness of the synthesized PDs was exploited for the detection of silver ions. Antimicrobial affinity of the synthesized PDs was estimated

via the inhibition zone technique with the evaluation of cell viability percentage. Eventually, the potentiality of the currently nucleated PDs based on CD as anti-inflammatory reagents was comparative study between ingraining of PDs under acidic versus basic conditions for clustering of cytotoxic PDs against breast cancer (MCF-7) was estimated with the WST-1 assay.

2. EXPERIMENTAL WORK

2.1. Materials and Chemicals. B-CD ($\geq 97\%$), magnesium chloride (MgCl_2 , 98%), potassium bromide (KBr, 99%), silver nitrate (AgNO_3 , 99%), zinc acetate [$\text{Zn}(\text{CH}_3\text{COO})_2$, 99%], copper nitrate [$\text{Cu}(\text{NO}_3)_2$, 99%], and cadmium nitrate ($\text{Cd}(\text{NO}_3)_2$, 99%) were purchased from Sigma-Aldrich. Sodium hydroxide (NaOH, 99%) and acetic acid (CH_3COOH , 99%) were supported by Merck, Darmstadt–Germany. All chemicals were exploited as received and prepared by using the deionized water.

2.2. Synthesis of Lipophobic QDs. In 1 L, 10 g of CD was dissolved under alkaline and acidic conditions, with 4% of NaOH (or acetic acid), while at 90 °C, the reaction liquor was left for 2 h under magnetic stirring. The solution color was observably altered to be yellowish in color. Afterward, in a vertical hydrothermal autoclave reactor, the reaction liquor was transferred in an oven for complete clustering of PDs at 140 and 190 °C for 6 h. The dark brown reaction liquor was cooled in atmospheric air to be centrifuged (at 5000 rpm for 20 min) to remove the undissolved particles (precipitate). Finally, the supernatants were dialyzed with distilled water by using Pur-A-Lyzer dialysis kits (MWCO 6–8 kDa from Sigma-Aldrich) to eliminate the enlarged particles and preserve the pure PDs for further analyses.

2.3. Instrumental Characterization. Absorption spectra for the prepared PDs colloids were manifested under UV–visible spectrophotometry (T80 UV-VIS, PG instruments Ltd) at 250–750 nm. Geometry and estimation of particle size for the prepared nano-colloids investigated via anticipating of high-resolution TEM from Japan (JEOL-JEM-1200). The particle size of PDs was estimated by 4 pi analysis software (from USA) for 50 particles at least. Under diffraction-limited spatial resolution in the range of 500–3500 cm^{-1} , the spectra were obtained. Infrared spectra were recorded using Jasco FT/IR 6100 spectrometer. The absorbance was detected in the range of 500–4000 cm^{-1} using 15 points smoothing, 4 cm^{-1} resolution, and 64 scanning times with a scanning rate of 2 mm s^{-1} . Spectral mapping of nuclear magnetic resonance (¹H NMR and ¹³C NMR) was detected on a Jeol-Ex-300 NMR spectrometer (JEOL-Japan). Photoluminescence for the synthesized PDs was monitored via spectro-fluorometer (JASCO FP8300). The measurements were performed at room temperature with excitation at 340 nm, while emission was estimated at room temperature.

2.4. Antimicrobial Affinity. Antimicrobial affinity of the clustered PDs against selected pathogens was affirmed using the Kirby–Bauer disk diffusion technique (inhibition zone technique).⁴⁷ In such an experimental test, three different pathogens of Gram-positive bacteria strain (*S. aureus*), Gram-negative bacteria strain (*Escherichia coli*), and fungal strain (*Candida albicans*) were selected for examination. In the mentioned test, different examined bacterial strains were promoted for growing in the medium for preparing pathogenic colloids. 100 μL of bacteria colloid was spread over agar plates corresponded to the broth to be tested. 10 μL of PDs was

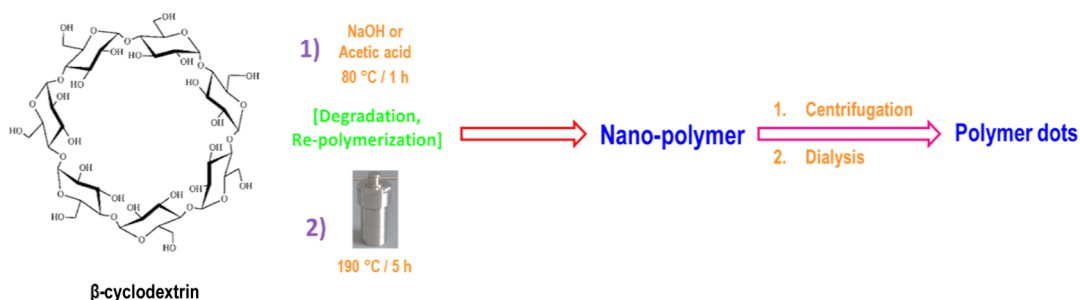


Figure 1. Scheme presented the preparation of PDs from β -CD.

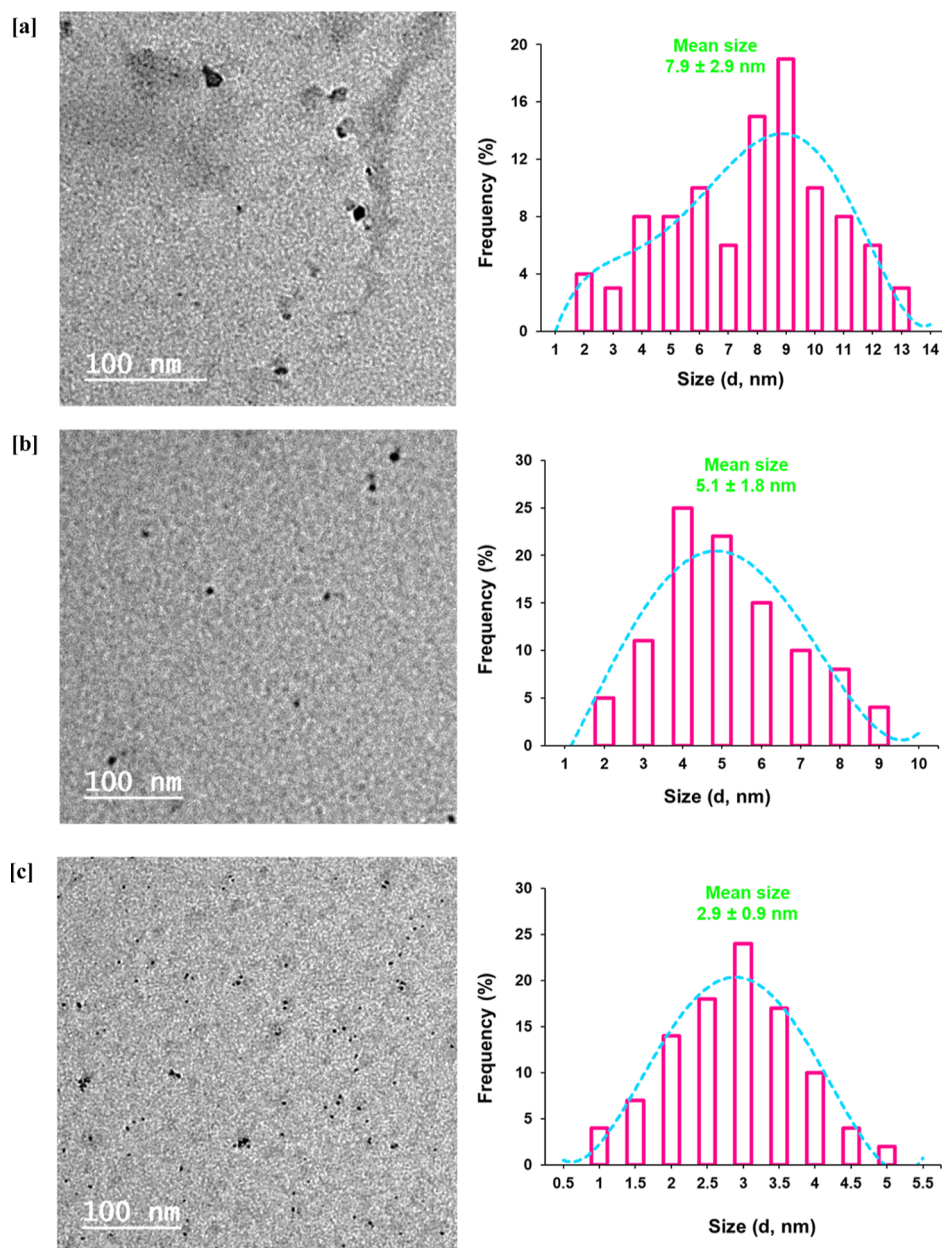


Figure 2. Transmission electron micro images for the prepared PDs and the corresponding particle size distribution; [a] 140 °C-NaOH, [b] 190 °C-NaOH, and [c] 190 °C-acetic.

dropped within the middle of plates for consequential incubation at 37 °C for 1 day. The diameter of the inhibition zone was estimated in mL with slipping calipers in accordance to NCCLS, 1997.⁴⁸

2.5. Anticancer Performance. Comparative study between ingrain of PDs under acidic versus basic conditions for clustering of cytotoxic PDs against breast cancer (MCF-7) was estimated with the WST-1 assay, which was proceeded in

Nawa Scientific Inc. (Mokatam, Egypt). The examined cells were dispersed in a DMEM medium supplemented with streptomycin (100 mg/mL), penicillin (100 units/mL), and heat-inactivated fetal bovine (10%) in humidified, atmospheric CO₂ [5% (v/v)] at 37 °C. Using Abcam kit (ab155902WST-1 Cell Proliferation Reagent), via the WST-1 assay, the cell mortal percentage was evaluated. 50 μ L of cell suspension (3×10^3 cells) was grown in 96-well plates for sequential incubation for 1 day. Afterward, curing of cells with another aliquot of PDs (50 μ L) at serial concentrations of 10–1000 μ g/mL was proceeded. After 2 days of exposing to PDs, cells were left for chemical interaction with WST-1 reagent (10 μ L) and the absorption was detected at 450 nm (using BMG LABTECH-FLUOstar Omega microplate reader, Allmendgrün, Ortenberg) after 1 h.⁴⁹

2.6. Florescent Detection of Ag Ions. The as-synthesized PDs were monitored for their luminescent sensitiveness to be applied for detecting heavy metals to act as luminescent metal detectors. With a concentration of 200 mM, Mg⁺, Cu⁺², Cd⁺², Ag⁺, Br⁻, and I⁻ ions were so-prepared. Utility of PDs as luminescent metal detector was performed in PBS buffer (pH 7.0) at room temperature. Whereas, PDs (0.5 mL) were added to metal salts (0.5 mM). The colloids were mixed, and after 1 h, at room temperature, the luminescence emission spectral data were estimated. PDs were exploited in the detection of Ag⁺ at different concentrations ranged in 0–2.5 mM. The photoluminescent detection was carried out using a spectro-fluorometer (JASCO FP8300) with excitation at 340 nm.

3. RESULTS AND DISCUSSION

3.1. Nucleation of Multifunctional Lipophobic PDs.

Implantation of multifunctional lipophobic PDs as bioactive/photoluminescent metal detectors was successively performed via facile/green procedure under the hydrothermal conditions from basic and acidic digested CD as schematically summarized in Figure 1. In accordance to literature, the mechanism for synthesis of the desired PDs was hypothesized as follows: first, CD macromolecular units are suggested to be digested under the effect of sodium hydroxide or acetic acid, under two chosen reaction temperatures: 140 and 190 °C. Sequentially, under the hydrothermal condition, re-polymerizing, aromatizing, and eventual oxidation were assumed to be proceeded to produce carbon nanostructures; either carbon nanoparticles (CNPs) or PDs.⁵⁰ Last, the prepared nano-colloids were dialyzed for ultra-purification to obtain mono-dispersed PDs with regulable topography.⁵⁰ CD was preliminary hydrolyzed into glucose, that further degraded into furfural moieties,^{51,52} that subsequently polymerized to produce the desired PDs (in the form of aromatic graphite sheets) as with surface decorative oxygen containing functional groups for tuning the color of digested CD colloidal solution to yellow and then to reddish brown color.^{53,54}

Geometrical features and topography of the clustered PDs under both acidic and basic conditions at 140 and 190 °C, and the micrographs of TEM are plotted in Figure 2, whereas, the size distribution was also estimated. The estimated data of particle size revealed that all of the clustered PDs were exhibited with smaller size less than 10 nm and spherical in shape. Under basic conditions, PDs with the largest particle size was nucleated at 140 °C (Figure 2a, 7.9 ± 2.9 nm), however, elevation of reaction temperature up to 190 °C resulted in the generation of more controllable/rationally

smaller-sized PDs with size distribution of 5.1 ± 1.8 nm (Figure 2b). However, processing the reaction under acidic conditions at 190 °C was shown to act in nucleation of CNPs (Figure 2c, 2.9 ± 0.9 nm), as supposed in the reaction mechanism, whereas acidification with elevated temperature resulted in vigorous deterioration of the polymeric blocks of CD to produce NPs rather than the desirable PDs.

Analysis of zeta electric potential was carried out for informing the zeta potential of the currently prepared nano-colloids under alkaline conditions compared to that nucleated under acidic conditions. Zeta potential is a significant parameter for the attraction or repulsive action between the nanostructures in colloids. The smaller the size of the suspended nanostructures, the greater is the detected negative values of the zeta potential, i.e., higher is the stability of the nano-colloid, as the stable colloidal suspension or dissolution could protect PDs from agglomeration. It could be observed from Figure S2, the detected negative charged value of zeta potential for both of nano-colloids prepared under both of acidic and basic conditions, to be ranged at –5 to –8 mV for nano-colloid prepared under acidic conditions, whereas it was estimated with higher negative value (–13 to –18 mV) in the case of nano-colloid prepared under basic conditions. This approves that nano-colloids prepared under basic conditions were exhibited with better physical stability rather than that prepared under acidic conditions.

The optical activities of PDs in grained from CD under both acidic and basic conditions at 140 and 190 °C are presented in Figure S2. The visual observation of the prepared sample solutions (Figure S2c) showed that the CQD colloid that was prepared under alkaline conditions at lower temperature of 140 °C was colorless, whereas elevation of the reaction temperature up to 190 °C resulted in the preparation of the PD colloid with a pale yellow color. However, performing the nucleation reaction under acidic conditions at 190 °C generated CNPs with the darkest reddish-brown color.

Figure S2a declared that, PD colloids prepared under basic conditions showed two characteristic absorbance peaks for CQDs; at 220 nm that is characteristic for π -electrons of the C=C aromatic sp² bond, i.e., π - π^* transition, and at 280 nm that is specified for n - π^* of C=O groups, respectively.^{55,56} PDs are known to be characterized with spherical geometry and are composed of aromatic sheets of carbon atoms to be highly regulated in the crystalline structure. However, under acidic conditions at 190 °C, CNPs were produced, while the as referred typical bands were blue-shifted to a longer wavelength due to vigorous deterioration of CD as previously mentioned in the as-previously illustrated data.

Figure S2b was also plotted to show the spectral data of the prepared nano-colloids for emission after excitation at 400 nm, whereas the mapping data showed that the PD colloid prepared under basic conditions at 190 °C was shown with maximum estimated emission at 450 nm. These findings could be illustrated in accordance to literature,⁵⁷ as the optical absorption spectral mapping data of the prepared PDs is mainly detected in the ultraviolet range, the absorbance spectral results are mainly related to PD luminescence that is principally attributed to the composition of the crystalline structure PDs with heteroatoms. Additionally, more controllable nucleation of PDs with highly oriented crystalline aromatic structure or graphite structure, mainly results in the estimation of the typical absorption bands of PDs with more intensity.^{58–64} Therefore, the most intense typical absorption

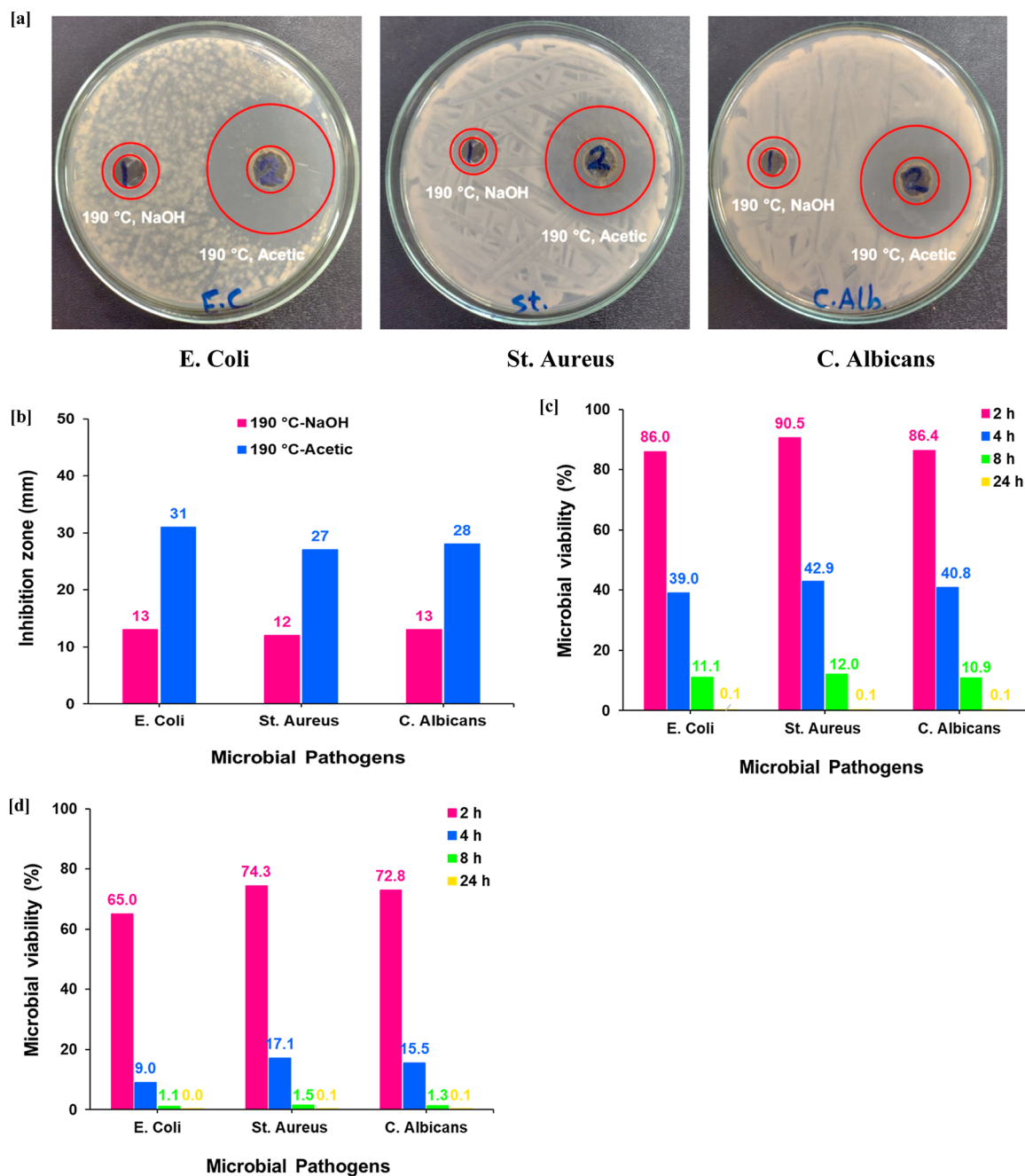


Figure 3. Antimicrobial efficiency for the prepared PDs; [a] photo images for the Petri-dishes with inhibition zones, [b] inhibition zone results, [c] microbial viability for 190 °C-NaOH, and [d] microbial viability for 190 °C-acetic.

spectra of CQDs were estimated for nano-colloid prepared under basic conditions at 190 °C to approve the compatibility of CD for successive nucleation of ultra-purified/monodispersed PDs organized in aromatic graphite sheets, with a controllable crystalline structure, under basic, hydrothermal conditions at 190 °C, which is in harmony with the above-illustrated data.^{58–64}

For verification of the chemical composition of the successively ingrained PDs, FT-IR spectral data for both pristine CD as well as all of the prepared PDs are presented in Figure S3, whereas the interpretation of the presented data was performed. Native CD spectrum exhibited with typical bands for the hydroxyl group and aliphatic group at 3292 and 2916 cm^{-1} , respectively. The spectral map also showed with

characteristic bands for free carboxyl groups, glycosidic bonds between monomeric units of gum macromolecules, and to pyranose ring at 1614, 1016, and at 851 cm^{-1} . Meanwhile, FT-IR spectra for the prepared nano-colloids showed that, the typical bands of CD were persisted after its exploitation for nucleation of PDs under basic conditions regardless of the reaction temperature. On the other side, the characteristic peaks for C=O become more intense, while that for OH still observed after exploitation of CD in preparation of the desired nano-colloids. Additionally, a new band weak characteristic band for un-substituted C=C bonds was detected at 2845 cm^{-1} . In addition, another band characteristic for the aromatic structure has been detected at 1588 cm^{-1} . However, under acidic conditions at elevated temperature at

190 °C, no IR bands were detected, meaning that a full deterioration of CD polymeric blocks was realized under such conditions.

¹H NMR spectral mapping results for nano-colloids prepared at 190 °C under both of acidic and basic conditions are shown in Figure S4 for more confirmable elucidation of the reaction mechanism of PDs clustering from CD macromolecular units under the hydrothermal condition. Figure S4a showed ¹H NMR for CQDs prepared from CD under basic conditions, while the spectrum for PDs exhibited with the typical bands for PDs at 1.8, 3.5–4, 4.5–5, and at 8.4 ppm, characteristic for protons of sp³ C–H, protons of O–H, protons bonded to C=O groups, and aromatic or sp² CH=CH protons, respectively. Whereas, such bands were similarly detected under acidic conditions with red-shifting (Figure S4b). Figure S4c,d is plotted for ¹³C NMR spectra PDs prepared under both acidic and basic conditions at 190 °C. It could be clearly observed that, the characteristic bands for PDs were detected at 24, 73, 170, and 174 ppm, corresponding to sp³ carbons, carbons attached with hydroxyl groups, C=C specialized for aromatic or sp² carbons and carbons of C=O groups.^{65,66}

All of the above-illustrated data approved the successive growth of PDs from alkali hydrolyzed CD under hydrothermal conditions through carbonization, cyclization, and aromatization for clustering of PDs (as graphite sheets) with oxygen-containing decorative groups which are responsible for the lipophobic potentiality of the clustered PDs.

3.2. Antimicrobial Potentiality of PDs. It was numerously reported that PDs are exhibited with antimicrobial potentiality against different microbial strains.^{67–72} In the current work, using the inhibition zone method, the antimicrobial potentiality for the clustered PDs at 190 °C under acidic (PDs-190 °C-acetic) and basic conditions (PDs-190 °C-NaOH) was studied against three microbial strains; Gram-positive bacteria (*S. aureus*), Gram-negative bacteria (*E. coli*), and fungi (*C. albicans*). Additionally, PDs microbial viability percent was also estimated. The evaluated data were presented in Figure 3. The figured-out data clearly revealed that, against all the tested microbial strains, PDs exhibited excellence in the antimicrobial action. Figure 3a,b showed that the PD colloid prepared under acidic conditions showed higher affinity rather than that nucleated under basic conditions; meanwhile, the inhibition zone diameter in the plates with *E. coli*, *S. aureus*, and *C. albicans* and incubated with PDs-190 °C-NaOH was evaluated to be 13, 12, and 13 mm, respectively. Whereas, the preparation of CQDs-190 °C-acetic showed superior antimicrobial affinity according to the estimated values of inhibition zone to be 31, 27, and 28 mm for *S. aureus*, *E. coli*, and *C. albicans*, respectively.

From Figure 3c,d, it could be depicted that the estimated microbial viability percent for the tested *E. coli*, *S. aureus*, and *C. albicans* that were incubated with PDs-190 °C-NaOH and CQDs-190 °C-acetic for only 4 h to be 39.0, 42.9, and 40.8 and 9.0, 17.1, and 15.5%, respectively. However, after incubation with PDs-190 °C-NaOH and PDs-190 °C-acetic after 24 h, microbial viability percentages were extensively diminished to be 0.1, 0.1, and 0.1 and 0, 0.1, and 0.1%, respectively. The estimated results are in accordance with that studied in literature,^{14,67,69,71,73} and the mechanism of the microbicidal action of the prepared PDs could be simply described in the following points;

- (i) The affinity of the prepared PDs as antimicrobial laborers is mainly attributed to their surface decoration with oxygen-containing groups.
- (ii) Decorative oxygen-based groups are responsible for the antimicrobial action of the clustered PDs against all the examined microbes through the liberation of ROS (reactive oxygen species).
- (iii) The generated ROS acted in extermination of the microbes, as ROS were easily entering through the microbial cell wall, leading to motivate the oxidative stress with deterioration of nucleic acids, to prohibit and distortion of the genes expression, mitochondria dysfunction, per-oxidization of lipids, inactivation of intracellular proteins, and decomposition of cell wall, resulting in apoptotic cell death.
- (iv) Both of the tested samples showed excellence in antimicrobial action; however, PDs-190 °C-acetic showed superiority in the antimicrobial potentiality that is logically attributed to the effectiveness of acidity in disinfection in addition to the effect of the dispersed PDs in the colloidal system.

Comparing to metallic nanostructural objects and metal-organic frameworks that were represented in different approaches,^{39–42} the currently synthesized nano-colloids were shown to exhibit the maximized antimicrobial affinity. This can approve the antimicrobial potentiality of the as-clustered PDs in addition to its biocompatibility and low toxicity. Therefore, it could be preferably applied as antimicrobial reagents more than metallic nanostructures for the medical and environmental applications.

3.3. Anticancer Affinity of PDs. Cell proliferation assay (WST-1) is one of the colorimetry estimation techniques and mainly relied on the chemical cleavage of tetrazolium salt (WST-1) under the effect of succinate-tetrazolium reductase from the respiratory chain of mitochondria in order to give formazan dye in living cells. Meaning that, higher the number of living cells, higher is the amount of the estimated formazan. Therefore, following up the effect of adding WST-1 for the detection of the formazan level in the examined cells is quantitative estimation for living cells. Currently, the cell proliferation assay was performed as a comparison study of PDs' anti-proliferative effects that were clustered under acidic conditions versus PDs prepared under basic conditions against a breast cancer (MCF-7) cell line. The cell mortality percent was estimated for breast cancer (MCF-7) after incubation with different concentrations of PDs that were implanted under acidic versus basic conditions.

Cytotoxic effects of a certain anticancer reagent meaning the motivation of necrosis, i.e., programmed cell death.⁷⁴ The cell mortality percent was estimated for the tested breast cancer cells (MCF-7) after treatment with PDs prepared under acidic and basic conditions, with different concentrations ranged in 0.1–1000 µg/mL (Figure S5). From the plotted results, treatment of examined cells with the prepared PDs for two days resulted in an unprecedented increase in cell mortality percent. Incubation of the tested cell PDs prepared under the basic condition with concentrations of 0.1, 10, and 100 µg/mL resulted in cell mortality percentages of 10, 25, and 30%, respectively. However, incubation of the tested cells with 1000 µg/mL of PDs prepared under basic and acidic conditions resulted in cell mortality percentages of 70 and 90%, respectively, to affirm the higher performance of PDs prepared

under acidic conditions as anticancer reagent. Additionally, estimation of IC₅₀ also affirmed the affinity of PDs ingrained under acidic conditions over that nucleated under basic conditions, whereas it was evaluated to be 88.6 and 232.5 $\mu\text{g}/\text{mL}$, respectively.

Anticancer and anti-proliferation actions of the clustered PDs in the current approach could be hypothesized as the clustered PDs with its free mobile electrons exhibited mortal effects against the examined cancer cells via the generation of ROS, while ROS acts in activating Caspase-3, that is identified as one of end proteases, an enzyme acts in controlling the necrosis and inflammation, as it essentially acts in deterioration of cell structure via degradation of the cytoskeletal proteins or fragmentation of nucleic acid.^{75,76} So, it could be summarized that, incubation of the tested cancer cell line with the currently nucleated PDs were mainly acted in the activation of Caspase-3 and consequently resulted in the eventual cell death.

The estimated data also revealed that, regardless of the concentration of the exploited PDs colloid as the anticancer laborer, PDs prepared under the acidic condition showed higher anticancer affinity compared to that prepared under the basic condition, which could be logically attributed to the acidosis effect of PDs ingrained under acidic conditions. Whereas, acidosis mainly affects in altering the cellular metabolic activities for the most of metabolites to be significantly reflected in metabolic disturbance. This alteration results in a decrement in cellular proliferation and increased the sensitivity of cells to ROS.

3.4. Optical Detection of Ag Ions in Aqueous Media.

One of the promising applicability of optically active PDs is to be exploited as environmental probes for the detection of different metal ions in aqueous media and in bio-sensing to evaluate the percentage of water contamination, so as it could be described as a feasible and environment friendly technique. Currently, the synthesized PDs, that were preliminary prepared at 190 °C under basic conditions were monitored for their fluorescence sensitivity in the detection of metal ions in aquatic media was systematically presented. The term in Figure 4 is fluorescence emission intensity of PDs (after excitation at 400 nm) was estimated in the absence and presence of metal ions [Mg^+ , Zn^{+2} , Cu^{+2} , Cd^{+2} , Ag^+ , and Br^-]. From the all examined metal ions, the optical sensitivity of the currently prepared PDs was maximized for Ag^+ ions. Fluorescence emission of PDs was mostly full quenched with 85 mM of Ag^+ ions. The key parameters for fluorescence intensity (F and F_0) with maximum excitation (400 nm) were further confirmed the highest affinity for fluorescence quenching by Ag^+ ions. Compared to various reports in literature, fluorescent PDs that were decorated with sulfur- or nitrogen-containing functional groups were sensitive to copper and ferric ions,^{77,78} while in the current approach, the ingrained PDs decorated with oxygen containing groups is optically sensitive for Ag^+ . The variability in the optical sensitivity of PDs for different metal ions is owing to the variation in the surface decorative groups⁷⁹ that is subsequently attributing to the interaction of silver ions with oxygen containing decorative groups of the currently exploited PDs. The optical quenching of metal ions that is relied on the concentration of the metal salt was performed for the affinity of CQDs-190 °C-NaOH in the detection of the selected metal ions in aquatic media (Figures S6 and S4). From Figure S6a, silver ions were shown to exhibit the maximized quenching of CQDs' fluorescence, whereas magnesium ions showed the minimized quenching of

CQDs' fluorescence with an emission intensity of 53 and the maximized quenching with an emission intensity of 20 for silver ions solution (Figure S6b). Additionally, by comparing between the absorbance spectrum of PDs-190 °C-NaOH (Figures S2a and S6c) that represented the absorbance for metal salt solutions after treating with PDs-190 °C-NaOH, it could be clearly observed that a third significant absorption band, identified as the surface plasmon resonance (SPR) band characteristic for AgNPs, was observed in the case of treating silver salt solution with the prepared CQDs-190 °C-NaOH. These finding could be interpreted that the treatment of silver salt solution with the as-prepared CQDs-190 °C-NaOH resulted in fluorescence quenching attributing to the chemical interaction between the nucleated PDs-190 °C-NaOH and silver ions to generate AgNPs that is approved via the spectral studies.

Figure 4 is represented for monitoring the effect of variation in Ag^+ ions concentration after treatment with the prepared PDs-190 °C-NaOH, it could be declared that, when the silver ions concentration was increased from 0.2 up to 2 mM, fluorescence quenching is increasing that is logically attributed to the chemical interaction between silver ions and PDs-190 °C-NaOH to liberate AgNPs (Figure 4a). Additionally, Figure 4b showed the effect of variation of silver salt concentration on the emission intensity to be gradually lowered with the increment of silver ions concentration to be minimized (15 mM) at the highest selected concentration of 2 mM. Figure 4c is plotted for the estimated data affirmed the linearity between the fluorescence of PDs and silver salt concentrations, whereas R^2 was quite high (coefficient determination = 0.9295). Moreover, the linearity in Figure 4c, can be easily exploited for estimation of the concentration of silver ions in different aqueous media via identifying the fluorescent intensity of PDs or from the estimated value of $1 - (F/F_0)$.

4. CONCLUSIONS

CD was currently exploited for implantation of PDs as bioactive laborers in order to be exploited as antimicrobial and anticancer reagents. Moreover, the implanted PDs was investigated to act as a safer alternative for metallic nanoparticles to act as environmental probes for the detection of metal ions in aquatic streams and attributing to their low toxic impact, less expensiveness, chemically inertness, bio-competence, and optical activities. Clustering of antimicrobial/florescent metal detector PDs with lipophobicity was currently carried out via a simple and green procedure. The effect for digestive fragmentation of CD under basic versus acidic conditions was systematically studied with following up the effect of the reaction temperature for the successive implantation of PDs with controllable topography and particle size. The successiveness of the current approach in clustering of PDs was confirmed via different instruments like, UV-visible spectroscopy, TEM, FT-IR, and NMR. Subsequently, the photoluminescence of the clustered PDs was also studied, while the superior optical sensitiveness of PDs were applied for detecting of silver ions. Antimicrobial affinity of the synthesized PDs was estimated via inhibition zone technique with evaluation of cell viability percentage. The estimated data revealed that, size average for PDs prepared under basic conditions (5.1 ± 1.8 nm) was clustered with a smaller size rather than that nucleated under acidic conditions (2.9 ± 0.9 nm). The synthesized PDs were exploited as florescent detectors in the estimation of Ag^+ ions in the aquatic streams.

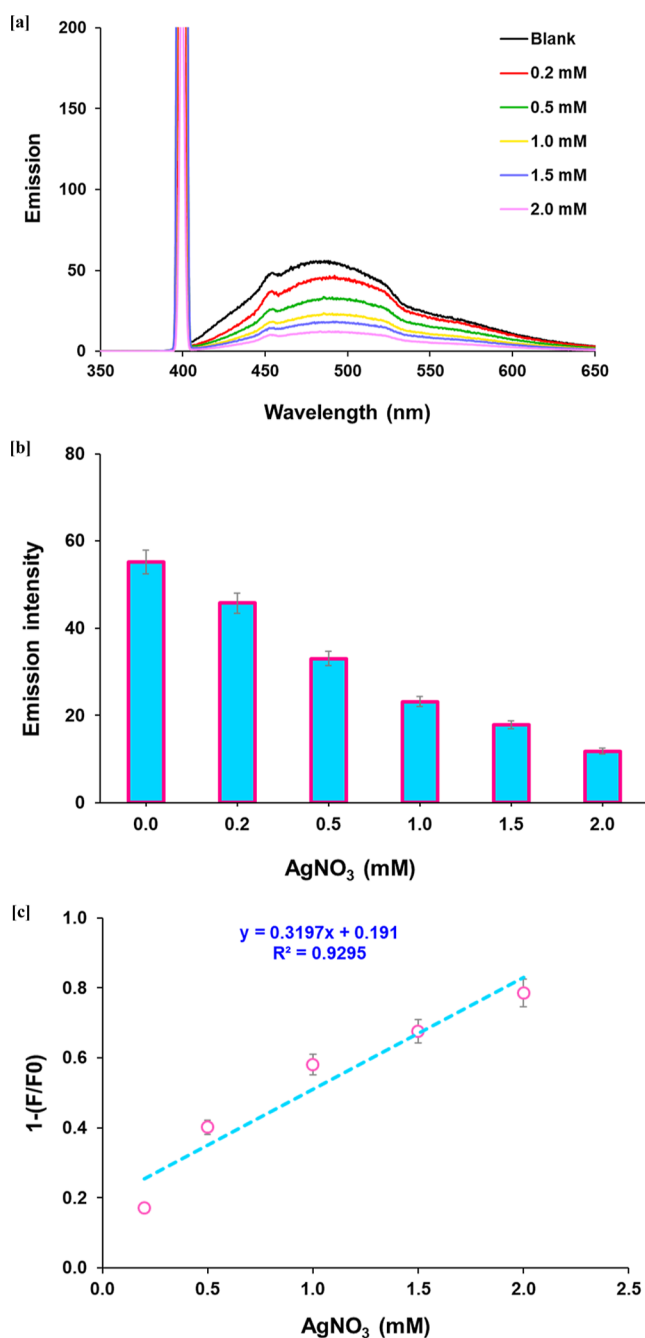


Figure 4. Detection of silver ion by the prepared PDs (190 °C-NaOH); [a] emission spectra, [b] fluorescence intensity, and [c] sensitivity of detection.

The prepared PDs were also advantageous with antimicrobial potentiality against *S. aureus* and *E. coli* and *C. albicans*. The cell viability percentage after 24 h was estimated to be 0.1% for PDs implanted under basic conditions toward *S. aureus* and *E. coli* and *C. albicans*. The anticancer affinity (against breast cancer, MCF-7) for PDs that implanted under acidic was (IC₅₀ 88.6 μg/mL) much higher than that obtained under basic conditions (IC₅₀ 232.5 μg/mL). The presented study approved the affinity of CD as an organic biopolymer for successive implantation of PDs exhibited with bioactivity and superiorly exploitable as environmental probes for the detection of silver ions in aquatic streams. The demonstrated technique could be ascribed as a simple and green procedure

for large scaled synthesis of biocide/florescent detector PDs instead of metallic nanoparticles for environmental purposes, without using organic solvents or toxic chemical reagents.

■ ASSOCIATED CONTENT

Supporting Information

The Supporting Information is available free of charge at <https://pubs.acs.org/doi/10.1021/acsomega.3c00873>.

Zeta potential, optical properties, infrared spectra, NMR spectra, anticancer activity, and emission detection for different ions (PDF)

■ AUTHOR INFORMATION

Corresponding Author

Nashwa M. El-Metwaly – Department of Chemistry, Faculty of Applied Sciences, Umm Al-Qura University, Makkah 21421, Saudi Arabia; Department of Chemistry, Faculty of Science, Mansoura University, Mansoura 35516, Egypt; orcid.org/0000-0002-0619-6206; Email: nmmohamed@uqu.edu.sa, n_elmetwaly00@yahoo.com

Authors

Albandary Almahri – Department of Chemistry, College of Science and Humanities in Al-Kharj, Prince Sattam Bin Abdulaziz University, Al-Kharj 11942, Saudi Arabia
Ameena M. Al-bonayan – Department of Chemistry, Faculty of Applied Sciences, Umm Al-Qura University, Makkah 21421, Saudi Arabia
Roba M. S. Attar – Department of Biology, College of Sciences, University of Jeddah, Jeddah 21959, Saudi Arabia
Alaa Karkashan – Department of Biology, College of Sciences, University of Jeddah, Jeddah 21959, Saudi Arabia
Basma Abbas – Department of Biology, College of Sciences, University of Jeddah, Jeddah 21959, Saudi Arabia
Salhah D. Al-Qahtani – Department of Chemistry, College of Science, Princess Nourah Bint Abdulrahman University, Riyadh 11671, Saudi Arabia

Complete contact information is available at:

<https://pubs.acs.org/10.1021/acsomega.3c00873>

Notes

The authors declare no competing financial interest.

The author(s) agree to publish the article under the Creative Commons Attribution License.

All data generated or analyzed during this study are included in this published article.

■ ACKNOWLEDGMENTS

Princess Nourah bint Abdulrahman University Researchers Supporting project number (PNURSP2023R122), Princess Nourah bint Abdulrahman University, Riyadh, Saudi Arabia.

■ REFERENCES

- (1) Liu, J.-H.; Wang, Y.; Yan, G.-H.; Yang, F.; Gao, H.; Huang, Y.; Wang, H.; Wang, P.; Yang, L.; Tang, Y.; et al. Systematic toxicity evaluations of high-performance carbon “quantum” dots. *J. Nanosci. Nanotechnol.* **2019**, *19*, 2130–2137.
- (2) Sun, S.; Zhang, L.; Jiang, K.; Wu, A.; Lin, H. Toward high-efficient red emissive carbon dots: facile preparation, unique properties, and applications as multifunctional theranostic agents. *Chem. Mater.* **2016**, *28*, 8659–8668.

- (3) Zheng, X. T.; Ananthanarayanan, A.; Luo, K. Q.; Chen, P. Glowing graphene quantum dots and carbon dots: properties, syntheses, and biological applications. *Small* **2015**, *11*, 1620–1636.
- (4) Baker, S. N.; Baker, G. A. Luminescent carbon nanodots: emergent nanolights. *Angew. Chem., Int. Ed.* **2010**, *49*, 6726–6744.
- (5) Wei, W.; Xu, C.; Ren, J.; Xu, B.; Qu, X. Sensing metal ions with ion selectivity of a crown ether and fluorescence resonance energy transfer between carbon dots and graphene. *Chem. Commun.* **2012**, *48*, 1284–1286.
- (6) Zhu, A.; Qu, Q.; Shao, X.; Kong, B.; Tian, Y. Carbon-dot-based dual-emission nanohybrid produces a ratiometric fluorescent sensor for in vivo imaging of cellular copper ions. *Angew. Chem., Int. Ed.* **2012**, *51*, 7185–7189.
- (7) Liu, C.; Zhang, P.; Zhai, X.; Tian, F.; Li, W.; Yang, J.; Liu, Y.; Wang, H.; Wang, W.; Liu, W. Nano-carrier for gene delivery and bioimaging based on carbon dots with PEI-passivation enhanced fluorescence. *Biomaterials* **2012**, *33*, 3604–3613.
- (8) Chen, P.-C.; Chen, Y.-N.; Hsu, P.-C.; Shih, C.-C.; Chang, H.-T. Photoluminescent organosilane-functionalized carbon dots as temperature probes. *Chem. Commun.* **2013**, *49*, 1639–1641.
- (9) Luo, P. G.; Sahu, S.; Yang, S.-T.; Sonkar, S. K.; Wang, J.; Wang, H.; LeCroy, G. E.; Cao, L.; Sun, Y.-P. Carbon “quantum” dots for optical bioimaging. *J. Mater. Chem. B* **2013**, *1*, 2116–2127.
- (10) Miao, P.; Han, K.; Tang, Y.; Wang, B.; Lin, T.; Cheng, W. Recent advances in carbon nanodots: synthesis, properties and biomedical applications. *Nanoscale* **2015**, *7*, 1586–1595.
- (11) Deng, Y.; Zhao, D.; Chen, X.; Wang, F.; Song, H.; Shen, D. Long lifetime pure organic phosphorescence based on water soluble carbon dots. *Chem. Commun.* **2013**, *49*, 5751–5753.
- (12) Qu, K.; Wang, J.; Ren, J.; Qu, X. Carbon dots prepared by hydrothermal treatment of dopamine as an effective fluorescent sensing platform for the label-free detection of iron (III) ions and dopamine. *Chem. Eur. J.* **2013**, *19*, 7243–7249.
- (13) Rastogi, A.; Pandey, F. P.; Hegde, G.; Manohar, R. Time-resolved fluorescence and UV absorbance study on *Elaeis guineensis*/oil palm leaf based carbon nanoparticles doped in nematic liquid crystals. *J. Mol. Liq.* **2020**, *304*, 112773.
- (14) Kováčová, M.; Špitálská, E.; Markovic, Z.; Špitálský, Z. Carbon Quantum Dots As Antibacterial Photosensitizers and Their Polymer Nanocomposite Applications. *Part. Part. Syst. Char.* **2020**, *37*, 1900348.
- (15) Zuo, P.; Lu, X.; Sun, Z.; Guo, Y.; He, H. A review on syntheses, properties, characterization and bioanalytical applications of fluorescent carbon dots. *Microchim. Acta* **2016**, *183*, 519–542.
- (16) Shi, W.; Wang, Q.; Long, Y.; Cheng, Z.; Chen, S.; Zheng, H.; Huang, Y. Carbon nanodots as peroxidase mimetics and their applications to glucose detection. *Chem. Commun.* **2011**, *47*, 6695–6697.
- (17) Yu, S.-J.; Kang, M.-W.; Chang, H.-C.; Chen, K.-M.; Yu, Y.-C. Bright fluorescent nanodiamonds: no photobleaching and low cytotoxicity. *J. Am. Chem. Soc.* **2005**, *127*, 17604–17605.
- (18) Yang, S.-T.; Cao, L.; Luo, P. G.; Lu, F.; Wang, X.; Wang, H.; Meziari, M. J.; Liu, Y.; Qi, G.; Sun, Y.-P. Carbon dots for optical imaging in vivo. *J. Am. Chem. Soc.* **2009**, *131*, 11308–11309.
- (19) Cao, L.; Wang, X.; Meziari, M. J.; Lu, F.; Wang, H.; Luo, P. G.; Lin, Y.; Harruff, B. A.; Veca, L. M.; Murray, D.; et al. Carbon dots for multiphoton bioimaging. *J. Am. Chem. Soc.* **2007**, *129*, 11318–11319.
- (20) Shamsipur, M.; Barati, A.; Karami, S. Long-wavelength, multicolor, and white-light emitting carbon-based dots: achievements made, challenges remaining, and applications. *Carbon* **2017**, *124*, 429–472.
- (21) Qiao, Z.-A.; Wang, Y.; Gao, Y.; Li, H.; Dai, T.; Liu, Y.; Huo, Q. Commercially activated carbon as the source for producing multicolor photoluminescent carbon dots by chemical oxidation. *Chem. Commun.* **2010**, *46*, 8812–8814.
- (22) Liu, H.; Ye, T.; Mao, C. Fluorescent carbon nanoparticles derived from candle soot. *Angew. Chem., Int. Ed.* **2007**, *46*, 6473–6475.
- (23) Tian, L.; Ghosh, D.; Chen, W.; Pradhan, S.; Chang, X.; Chen, S. Nanosized carbon particles from natural gas soot. *Chem. Mater.* **2009**, *21*, 2803–2809.
- (24) Zhou, J.; Booker, C.; Li, R.; Zhou, X.; Sham, T.-K.; Sun, X.; Ding, Z. An electrochemical avenue to blue luminescent nanocrystals from multiwalled carbon nanotubes (MWCNTs). *J. Am. Chem. Soc.* **2007**, *129*, 744–745.
- (25) Zhao, Q.-L.; Zhang, Z.-L.; Huang, B.-H.; Peng, J.; Zhang, M.; Pang, D.-W. Facile preparation of low cytotoxicity fluorescent carbon nanocrystals by electrooxidation of graphite. *Chem. Commun.* **2008**, *41*, 5116–5118.
- (26) Wu, Z. L.; Gao, M. X.; Wang, T. T.; Wan, X. Y.; Zheng, L. L.; Huang, C. Z. A general quantitative pH sensor developed with dicyandiamide N-doped high quantum yield graphene quantum dots. *Nanoscale* **2014**, *6*, 3868–3874.
- (27) Pan, D.; Zhang, J.; Li, Z.; Wu, M. Hydrothermal route for cutting graphene sheets into blue-luminescent graphene quantum dots. *Adv. Mater.* **2010**, *22*, 734–738.
- (28) Yang, Y.; Cui, J.; Zheng, M.; Hu, C.; Tan, S.; Xiao, Y.; Yang, Q.; Liu, Y. One-step synthesis of amino-functionalized fluorescent carbon nanoparticles by hydrothermal carbonization of chitosan. *Chem. Commun.* **2012**, *48*, 380–382.
- (29) Zhu, H.; Wang, X.; Li, Y.; Wang, Z.; Yang, F.; Yang, X. Microwave synthesis of fluorescent carbon nanoparticles with electrochemiluminescence properties. *Chem. Commun.* **2009**, *34*, 5118–5120.
- (30) Wang, Q.; Liu, X.; Zhang, L.; Lv, Y. Microwave-assisted synthesis of carbon nanodots through an eggshell membrane and their fluorescent application. *Analyst* **2012**, *137*, 5392–5397.
- (31) Villalonga, R.; Cao, R.; Fragoso, A. Supramolecular chemistry of cyclodextrins in enzyme technology. *Chem. Rev.* **2007**, *107*, 3088–3116.
- (32) Puskás, I.; Szemjonov, A.; Fenyvesi, É.; Malanga, M.; Szente, L. Aspects of determining the molecular weight of cyclodextrin polymers and oligomers by static light scattering. *Carbohydr. Polym.* **2013**, *94*, 124–128.
- (33) Ghatee, M. H.; Sedghamiz, T. Chiral recognition of Propranolol enantiomers by β -Cyclodextrin: Quantum chemical calculation and molecular dynamics simulation studies. *Chem. Phys.* **2014**, *445*, 5–13.
- (34) Prochowicz, D.; Kornowicz, A.; Lewiński, J. Interactions of native cyclodextrins with metal ions and inorganic nanoparticles: fertile landscape for chemistry and materials science. *Chem. Rev.* **2017**, *117*, 13461–13501.
- (35) Zhou, J.; Yang, Y.; Zhang, C.-y. Toward biocompatible semiconductor quantum dots: from biosynthesis and bioconjugation to biomedical application. *Chem. Rev.* **2015**, *115*, 11669–11717.
- (36) Yao, J.; Yang, M.; Duan, Y. Chemistry, biology, and medicine of fluorescent nanomaterials and related systems: new insights into biosensing, bioimaging, genomics, diagnostics, and therapy. *Chem. Rev.* **2014**, *114*, 6130–6178.
- (37) Bera, D.; Qian, L.; Tseng, T.-K.; Holloway, P. H. Quantum dots and their multimodal applications: a review. *Materials* **2010**, *3*, 2260–2345.
- (38) Szejtli, J. Introduction and general overview of cyclodextrin chemistry. *Chem. Rev.* **1998**, *98*, 1743–1754.
- (39) Emam, H. E.; Ahmed, H. B.; El-Deib, H. R.; El-Dars, F. M.; Abdelhameed, R. M. Non-invasive route for desulfurization of fuel using infrared-assisted MIL-53 (Al)-NH₂ containing fabric. *J. Colloid Interface Sci.* **2019**, *556*, 193–205.
- (40) Emam, H. E.; Zahran, M.; Ahmed, H. B. Generation of biocompatible nanogold using H₂O₂–starch and their catalytic/antimicrobial activities. *Eur. Polym. J.* **2017**, *90*, 354–367.
- (41) Ahmed, H. B.; Attia, M. A.; El-Dars, F. M.; Emam, H. E. Hydroxyethyl cellulose for spontaneous synthesis of antipathogenic nanostructures: (Ag & Au) nanoparticles versus Ag-Au nano-alloy. *Int. J. Biol. Macromol.* **2019**, *128*, 214–229.

- (42) Emam, H. E.; Darwesh, O. M.; Abdelhameed, R. M. In-growth metal organic framework/synthetic hybrids as antimicrobial fabrics and its toxicity. *Colloids Surf, B* **2018**, *165*, 219–228.
- (43) Pidot, S. J.; Gao, W.; Buultjens, A. H.; Monk, I. R.; Guerillot, R.; Carter, G. P.; Lee, J. Y.; Lam, M. M.; Grayson, M. L.; Ballard, S. A.; et al. Increasing tolerance of hospital *Enterococcus faecium* to handwash alcohols. *Sci. Transl. Med.* **2018**, *10*, No. eaar6115.
- (44) Tchounwou, P. B.; Yedjou, C. G.; Patlolla, A. K.; Sutton, D. J. Heavy metal toxicity and the environment. In *Molecular, clinical and environmental toxicology*; Springer, 2012; pp 133–164.
- (45) Singh, R.; Gautam, N.; Mishra, A.; Gupta, R. Heavy metals and living systems: An overview. *Indian J. Pharmacol.* **2011**, *43*, 246.
- (46) Yoo, D.; Park, Y.; Cheon, B.; Park, M.-H. Carbon dots as an effective fluorescent sensing platform for metal ion detection. *Nanoscale Res. Lett.* **2019**, *14*, 272.
- (47) Bauer, A. W.; Kirby, W. M. M.; Sherris, J. C.; Turck, M. Antibiotic susceptibility testing by a standardized single disc method. *Am. J. Clin. Pathol.* **1966**, *45*, 493–496.
- (48) CLSI. *Methods for Dilution Antimicrobial Susceptibility Tests for Bacteria That Grow Aerobically*; Approved Standard—9 Ed.; M07-A9 Clinical and Laboratory Standards Institute USA, 2012; Vol. 32 No. 2.
- (49) Alaifi, O. M.; Noorwali, A.; Zahran, F.; Al-Abd, A. M.; Al-Attas, S. Cytotoxicity of thymoquinone alone or in combination with cisplatin (CDDP) against oral squamous cell carcinoma in vitro. *Sci. Rep.* **2017**, *7*, 13131.
- (50) Li, H.; Ming, H.; Liu, Y.; Yu, H.; He, X.; Huang, H.; Pan, K.; Kang, Z.; Lee, S.-T. Fluorescent carbon nanoparticles: electrochemical synthesis and their pH sensitive photoluminescence properties. *New J. Chem.* **2011**, *35*, 2666–2670.
- (51) Ryu, J.; Suh, Y.-W.; Suh, D. J.; Ahn, D. J. Hydrothermal preparation of carbon microspheres from mono-saccharides and phenolic compounds. *Carbon* **2010**, *48*, 1990–1998.
- (52) Kwon, W.; Do, S.; Rhee, S.-W. Formation of highly luminescent nearly monodisperse carbon quantum dots via emulsion-templated carbonization of carbohydrates. *RSC Adv.* **2012**, *2*, 11223–11226.
- (53) Sakaki, T.; Shibata, M.; Miki, T.; Hirose, H.; Hayashi, N. Reaction model of cellulose decomposition in near-critical water and fermentation of products. *Bioresour. Technol.* **1996**, *58*, 197–202.
- (54) Chen, B.; Li, F.; Li, S.; Weng, W.; Guo, H.; Guo, T.; Zhang, X.; Chen, Y.; Huang, T.; Hong, X.; et al. Large scale synthesis of photoluminescent carbon nanodots and their application for bioimaging. *Nanoscale* **2013**, *5*, 1967–1971.
- (55) Kim, Y. J.; Guo, P.; Schaller, R. D. Aqueous Carbon Quantum Dot-Embedded PC60-PC61BM Nanospheres for Ecological Fluorescent Printing: Contrasting Fluorescence Resonance Energy-Transfer Signals between Watermelon-like and Random Morphologies. *J. Phys. Chem. Lett.* **2019**, *10*, 6525–6535.
- (56) Luo, Z.; Lu, Y.; Somers, L. A.; Johnson, A. T. C. High yield preparation of macroscopic graphene oxide membranes. *J. Am. Chem. Soc.* **2009**, *131*, 898–899.
- (57) Gao, X.; Du, C.; Zhuang, Z.; Chen, W. Carbon quantum dot-based nanoprobe for metal ion detection. *J. Mater. Chem. C* **2016**, *4*, 6927–6945.
- (58) Chae, A.; Choi, Y.; Jo, S.; Nur'aeni, N.; Paoprasert, P.; Park, S. Y.; In, I. Microwave-assisted synthesis of fluorescent carbon quantum dots from an A₂/B₃ monomer set. *RSC Adv.* **2017**, *7*, 12663–12669.
- (59) Pires, N. R.; Santos, C. M.; Sousa, R. R.; Paula, R.; Cunha, P. L.; Feitosa, J. Novel and fast microwave-assisted synthesis of carbon quantum dots from raw cashew gum. *J. Braz. Chem. Soc.* **2015**, *26*, 1274–1282.
- (60) Zuo, J.; Jiang, T.; Zhao, X.; Xiong, X.; Xiao, S.; Zhu, Z. Preparation and application of fluorescent carbon dots. *J. Nanomater.* **2015**, *2015*, 1–13.
- (61) Chandra, S.; Pathan, S. H.; Mitra, S.; Modha, B. H.; Goswami, A.; Pramanik, P. Tuning of photoluminescence on different surface functionalized carbon quantum dots. *RSC Adv.* **2012**, *2*, 3602–3606.
- (62) Gao, J.; Zhu, M.; Huang, H.; Liu, Y.; Kang, Z. Advances, challenges and promises of carbon dots. *Inorg. Chem. Front.* **2017**, *4*, 1963–1986.
- (63) Liu, X.; Pang, J.; Xu, F.; Zhang, X. Simple approach to synthesize amino-functionalized carbon dots by carbonization of chitosan. *Sci. Rep.* **2016**, *6*, 31100.
- (64) Song, J.; Zhao, L.; Wang, Y.; Xue, Y.; Deng, Y.; Zhao, X.; Li, Q. Carbon quantum dots prepared with chitosan for synthesis of CQDs/AuNPs for iodine ions detection. *Nanomaterials* **2018**, *8*, 1043.
- (65) Emam, H. E.; Ahmed, H. B. Antitumor/antiviral carbon quantum dots based on carrageenan and pullulan. *Int. J. Biol. Macromol.* **2021**, *170*, 688–700.
- (66) Emam, H. E.; El-Shahat, M.; Hasanin, M. S.; Ahmed, H. B. Potential military cotton textiles composed of carbon quantum dots clustered from 4-(2, 4-dichlorophenyl)-6-oxo-2-thioxohexahydroprymidine-5-carbonitrile. *Cellulose* **2021**, *28*, 9991–10011.
- (67) Li, H.; Huang, J.; Song, Y.; Zhang, M.; Wang, H.; Lu, F.; Huang, H.; Liu, Y.; Dai, X.; Gu, Z.; et al. Degradable carbon dots with broad-spectrum antibacterial activity. *ACS Appl. Mater. Interfaces* **2018**, *10*, 26936–26946.
- (68) Li, Y. J.; Harroun, S. G.; Su, Y. C.; Huang, C. F.; Unnikrishnan, B.; Lin, H. J.; Lin, C. H.; Huang, C. C. Synthesis of self-assembled spermidine-carbon quantum dots effective against multidrug-resistant bacteria. *Adv. Healthcare Mater.* **2016**, *5*, 2545–2554.
- (69) Dong, X.; Liang, W.; Meziani, M. J.; Sun, Y.-P.; Yang, L. Carbon dots as potent antimicrobial agents. *Theranostics* **2020**, *10*, 671–686.
- (70) Marković, Z. M.; Jovanović, S. P.; Mašković, P. Z.; Danko, M.; Mičušik, M.; Pavlović, V. B.; Milivojević, D. D.; Kleinová, A.; Špitalský, Z.; Todorović Marković, B. M. Photo-induced antibacterial activity of four graphene based nanomaterials on a wide range of bacteria. *RSC Adv.* **2018**, *8*, 31337–31347.
- (71) Stanković, N. K.; Bodik, M.; Šiffalović, P.; Kotlar, M.; Mičušik, M.; Špitalsky, Z.; Danko, M.; Milivojević, D. D.; Kleinová, A.; Kubat, P.; et al. Antibacterial and antibiofouling properties of light triggered fluorescent hydrophobic carbon quantum dots Langmuir–Blodgett thin films. *ACS Sustain. Chem. Eng.* **2018**, *6*, 4154–4163.
- (72) Kováčová, M.; Marković, Z. M.; Humpolíček, P.; Mičušik, M.; Švajdlenková, H.; Kleinová, A.; Danko, M.; Kubat, P.; Vajdák, J.; Capakova, Z.; et al. Carbon quantum dots modified polyurethane nanocomposite as effective photocatalytic and antibacterial agents. *ACS Biomater. Sci. Eng.* **2018**, *4*, 3983–3993.
- (73) Ristic, B. Z.; Milenkovic, M. M.; Dakic, I. R.; Todorovic-Markovic, B. M.; Milosavljevic, M. S.; Budimir, M. D.; Paunovic, V. G.; Dramicanin, M. D.; Markovic, Z. M.; Trajkovic, V. S. Photodynamic antibacterial effect of graphene quantum dots. *Biomaterials* **2014**, *35*, 4428–4435.
- (74) Arkan, E.; Barati, A.; Rahmanpanah, M.; Hosseinzadeh, L.; Moradi, S.; Hajjalyani, M. Green synthesis of carbon dots derived from walnut oil and an investigation of their cytotoxic and apoptogenic activities toward cancer cells. *Adv. Pharm. Bull.* **2018**, *8*, 149–155.
- (75) Elmore, S. Apoptosis: a review of programmed cell death. *Toxicol. Pathol.* **2007**, *35*, 495–516.
- (76) Milner, A.; Palmer, D.; Hodgkin, E.; Eliopoulos, A.; Knox, P.; Poole, C.; Kerr, D.; Young, L. Induction of apoptosis by chemotherapeutic drugs: the role of FADD in activation of caspase-8 and synergy with death receptor ligands in ovarian carcinoma cells. *Cell Death Differ.* **2002**, *9*, 287–300.
- (77) Wu, H.; Jiang, J.; Gu, X.; Tong, C. Nitrogen and sulfur codoped carbon quantum dots for highly selective and sensitive fluorescent detection of Fe (III) ions and L-cysteine. *Microchim. Acta* **2017**, *184*, 2291–2298.
- (78) Zhao, L.; Li, H.; Xu, Y.; Liu, H.; Zhou, T.; Huang, N.; Li, Y.; Ding, L. Selective detection of copper ion in complex real samples based on nitrogen-doped carbon quantum dots. *Anal. Bioanal. Chem.* **2018**, *410*, 4301–4309.
- (79) Algarra, M.; Campos, B. B.; Radotić, K.; Mutavdžić, D.; Bandosz, T.; Jiménez-Jiménez, J.; Rodríguez-Castellón, E.; Esteves da Silva, J. C. G. Luminescent carbon nanoparticles: effects of chemical functionalization, and evaluation of Ag⁺ sensing properties. *J. Mater. Chem.* **2014**, *2*, 8342–8351.